Dry mechanosynthesis and characterization of carbonate apatite based on Indonesian natural sources

Cite as: AIP Conference Proceedings **2349**, 020072 (2021); https://doi.org/10.1063/5.0052812
Published Online: 24 June 2021

Herlina Damayanti, Kristanto Wahyudi, Karlina Noordiningsih, Ayu Ratnasari, and Devi Rianti

Dry Mechanosynthesis and Characterization of Carbonate Apatite Based on Indonesian Natural Sources

Herlina Damayanti[1, a)], Kristanto Wahyudi[1], Karlina Noordiningsih[1], Ayu Ratnasari[1], and Devi Rianti[2]

[1]*Center for Ceramics, Ministry of Industry, Indonesia*
[2]*Faculty of Dentistry, Airlangga University, Indonesia*

[a)]Corresponding author: herlinadamayanti49@gmail.com

Abstract. Synthetic carbonate apatite is generally used in bone tissue engineering because of their similar chemical composition with the inorganic component of hard tissue. In natural hard tissue, apatite is supplemented by tracing ions such as carbonate. Carbonate apatite is more bioactive than stoichiometric hydroxyapatite. In this study, carbonate apatite powders were prepared by dry mechanosynthesis method, the powder mixture of hydroxyapatite (HA) powders from Center for Ceramic based on Indonesian limestone and carbonate sources came from $CaCO_3$ (Cirebon origin) and $MgCO_3$. The synthesized results were characterized by X-ray diffraction (XRD), X-ray fluorescence (XRF), Fourier-transform infrared spectroscopy (FTIR), and scanning electron microscopy (SEM). The dry mechanosynthesis method produced carbonate apatite, which is formed by a solid-solid reaction between hydroxyapatite and carbonate sources. The XRD patterns peaks around 31.6 - 33^o confirmed the formation of the apatite phase. Based on FTIR spectra, the mixture of HA and $MgCO_3$ forms type B of carbonate apatite as predominant and type A is not dominant. SEM image shows that the particles have an irregular shape with interconnected agglomeration between fine particles to form large particles. Hence, dry mechanosynthesis is a simple method to produce carbonate apatite from Indonesian natural sources. Moreover, this method can reduce waste and cost during production.

INTRODUCTION

The synthesis of biomaterials, especially bioceramic for bone reconstruction, remains the most interesting object in the research technology development. One of these materials is hydroxyapatite ($Ca_{10}(PO_4)_6(OH)_2$), which is highly biocompatible with the human body. Hydroxyapatite, as a bioceramic, had chemical and crystallographic similar to inorganic components found in hard tissue (teeth and bones) [1]. However, there is a different composition between stoichiometric hydroxyapatite and human bone minerals, which is a carbonate component in human bone minerals [2]. Carbonate is abundant impurity ions about 4-8% [3–5]. The addition of carbonate to hydroxyapatite can affect its properties, such as an increase in solubility, a decrease in crystallinity, a change in crystal morphology, and an increase of chemical reactivity due to the weak bonding [6–8]. For this reason, the main target of this research is the preparation of a synthetic carbonate apatite as bone-substitute ceramics, which resembles the chemical composition of natural hard tissues. Carbonate apatite is similar to the inorganic component of natural bone and it is a more desirable bioactive material than stoichiometric hydroxyapatite [9].

In this study, the source of carbonate ions added to hydroxyapatite is calcium carbonate ($CaCO_3$) and magnesium carbonate ($MgCO_3$). It has been reported that $CaCO_3$ is a potential inorganic precursor to induce bone mineral formation [10–12]. Several studies on the preparation of carbonate apatite also used $CaCO_3$ as a precursor material [7,13–18]. Moreover, $CaCO_3$ is also one of the most plentiful minerals in nature [19]. Magnesium (Mg) is one of the ions contained in natural apatite with high concentrations of cartilage and natural bone tissue during the initial phases of osteogenesis and tends to disappear when the bone is mature [20]. Mg ion can also accelerate nucleation kinetics and

4th International Seminar on Chemistry
AIP Conf. Proc. 2349, 020072-1–020072-6; https://doi.org/10.1063/5.0052812
Published by AIP Publishing. 978-0-7354-4100-2/$30.00

retards the crystallinity of hydroxyapatite [21–23]. It has been reported by several authors that the addition of Mg and CO_3 ions to hydroxyapatite can increase osteoblast adhesion, proliferation, and metabolic activation [24–26].

Carbonate apatites have been successfully produced by the dry mechanosynthesis route [16,17,27]. Dry mechanosynthesis is carried out in solid-state reactions are activated by mechanical milling, where it involves the dispersion of solids and their plastic deformation [28,29]. Mechanical milling is carried out in milling tools (such as pot mill, planetary mill, ball mill, etc.). In a mill, reactants are broken by collisions between balls or balls and walls. Reagents absorb part of the energy provided by the collisions or frictions for the reaction needed [30].

This study aims to produce carbonate apatite based on Indonesian natural materials with an easy and economical method. This paper reports the synthesis of carbonate apatite-based hydroxyapatite, which has been developed by the Center for Ceramics [31] and the carbonate source from $CaCO_3$ / $MgCO_3$ by dry mechano-method. This method and materials be the main idea to produce carbonate apatite in this study.

MATERIALS AND METHOD

The initial hydroxyapatite was obtained from hydroxyapatite synthesis by wet precipitation method and based on Indonesian limestone [31]. Carbonate sources came from $CaCO_3$ (Cirebon origin) and $MgCO_3$ (supplied by Brataco). Dry mechanosynthesis was applied to materials of single hydroxyapatite (HA 48), mixing between hydroxyapatite and $CaCO_3$ with ratio 6.67:1 (HC 48), and mixing between hydroxyapatite and $MgCO_3$ with ratio 6.67:1 (HM 48).

Each material was milling in the porcelain pot mill 5 kg, porcelain milling balls size 25 mm – 30 mm, and weight ratio between materials and balls milling 1:1. In this study, dry mechanosynthesis processed by rotation speed 80 rpm in the interval 48 h were studied to compare the effect of carbonate material on the carbonated apatite formation.

Characterization

Crystal phases identification was carried out by X-ray powder diffraction (XRD) technique using a Philips Xpert MPD diffractometer equipped with Cu incident radiation (40 kV, 30 mA). The broad-angle diffraction patterns were collected at -275.15°C over the range of 5–60°. Scanning Electron Microscope JEOL JSM-6360LA, equipped with Energy Dispersive System (EDS), is used to characterize the microstructure of carbonate apatite. The sample was cut into blocks and then coated with conductive electron dotite. The sample was measured with a voltage of 15kV and a magnification of 5000x. Fourier transform infrared spectrophotometer (FTIR), Thermo Scientific Nicolet iS10 recorded the vibration spectra using the region 4000, absolute region 99.487, wavelength 4000-500, and threshold 50.

RESULTS AND DISCUSSION

The experimental XRD pattern of all milled and unmilled materials is shown in Figure 1. Figure 1 (a) exhibited the HA phase with sharp diffraction peaks without the impurity phase from basic materials (HA Center for Ceramic). It indicates that the HA structure has high crystallinity. High peaks around 31.6 – 33° indicate the formation of an appetite phase. The intensity of the HA peaks decreases after the grinding process is shown in Figure 1 (b), 1 (c), and 1 (d). The intensity at highest peak 31.7° decrease due to milling effect that is 492 at HA unmilled, 423 at HA milled, 407 at HM 48, and 373 at HC 48. After 48 hours of milling, basic materials (HA) and the powder mixtures (HA and $MgCO_3$) produce a single-phase HA formation, free from impurities that come from raw material or milling media. The undetectable presence of Mg in the XRD pattern may be due to a complete reaction by mechanical activation. Conversely, the presence of $CaCO_3$ is shown in Figure 1 (d) as the second phase. Therefore, decreasing the apatite phase intensity in HC 48 due to the formation of the second phase. This result indicated that monophasic apatite might be obtained by this method from a mixture with a stoichiometric Ca/P ratio 1.67 of the stoichiometry HA, considering that the addition of $CaCO_3$ will cause an excess of Ca [32].

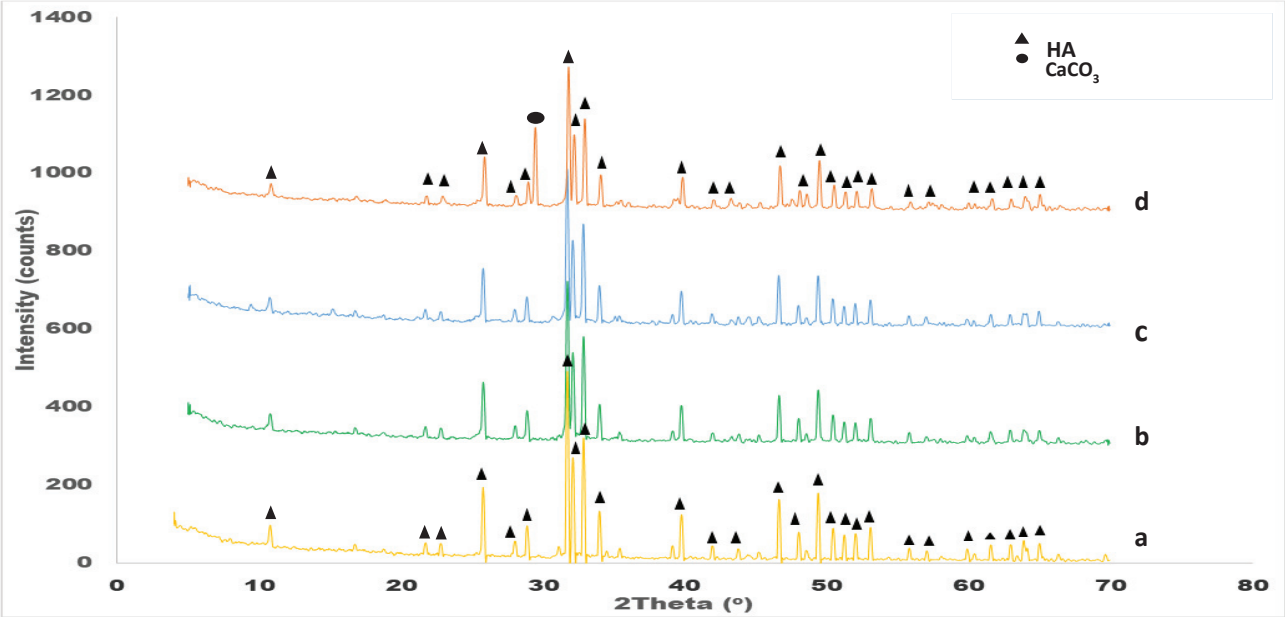

FIGURE 1. XRD pattern of all milled and unmilled materials: (a) HA unmilled, (b) HA milled, (c) HM 48, and (d) HC 48

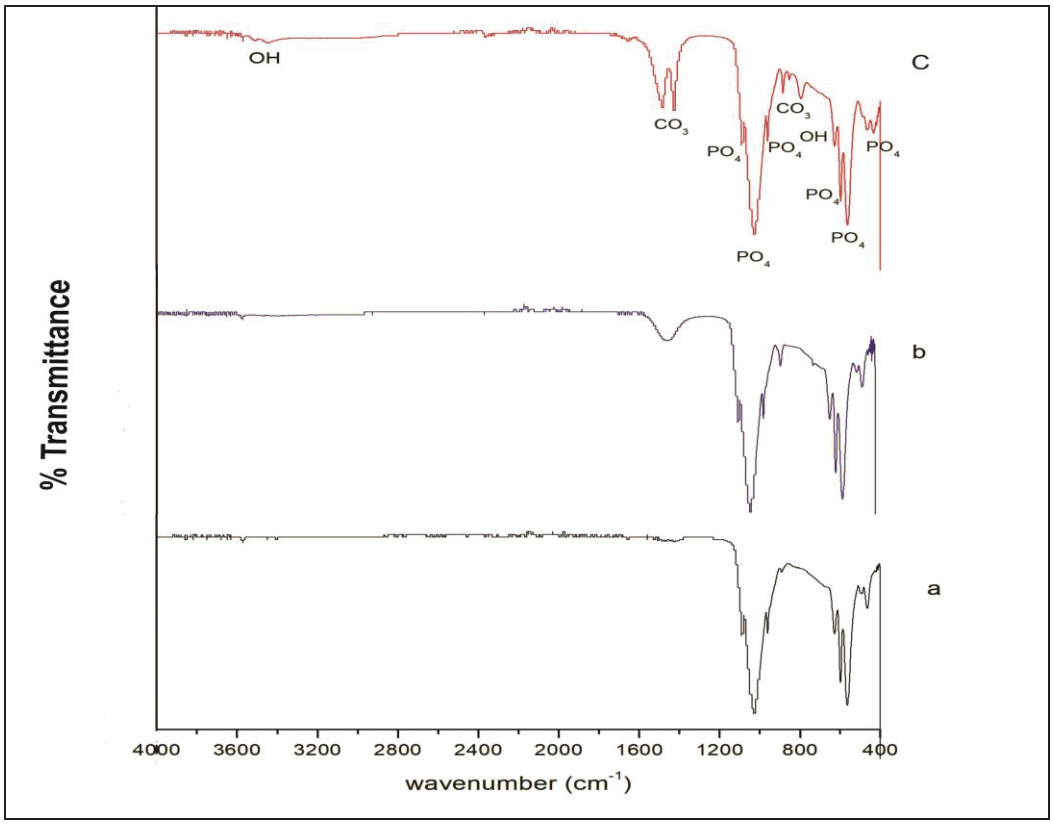

FIGURE 2. FTIR spectra of milled materials: (a) HA 48, (b) HC 48, (c) HM 48

Figure 2 shows FTIR spectra of milled HA powders either with or without carbonate source addition. As shown in Figure 2, different vibrational modes of the phosphate (PO_4^{3-}) and hydroxyl (OH^-) groups associated with HA.

The spectra in Figure 2 (c) indicated the typical carbonate apatite. The vibration band at 467 cm^{-1} in the spectrum is the result of PO_4 stretching (v_2) mode. The doublets at 563 and 598 cm^{-1} are the result of PO_4 bending (v_4) vibration. The 961 cm^{-1} vibration band is related to the symmetric stretching (v_1) vibration of P-O bonds. Furthermore, the strong bands at 1026 and 1086 are derived from P-O stretching (v_3) vibration [17,33–35]. Type B carbonate is shown in a doublet band at 1484 and 1425 cm^{-1} as stretching (v_3) vibration and a single band at 881 cm^{-1} that out-of-plane bending vibration (v_2). It indicates the substitution of carbonate ion into the apatite structure at the phosphate ion position is predominant. On the other hand, the band at 884 and a weak band at 1653 cm^{-1} exhibited type A carbonate that formed when hydroxyl groups are replaced by carbonate groups [14,18,36–38]. The stretching vibration of hydroxyl groups was detected at 627 cm^{-1}. The weak absorption around 3568 cm^{-1} reflected the vibration of hydroxyl [7,13].

The morphology of all milled sample was characterized by SEM technique. As shown in Figure 3, random agglomerated particles are formed with a size of about 0.3-1.6 µm. The resulting particles have an irregular shape, which fine agglomerates interconnected in different ways into different structures formed large agglomerates. The addition of carbonate ions making the nuclei size of apatite smaller and decrease the crystallization corresponding to XRD pattern. Figure 3 shows SEM images of HM and HC smaller than HA.

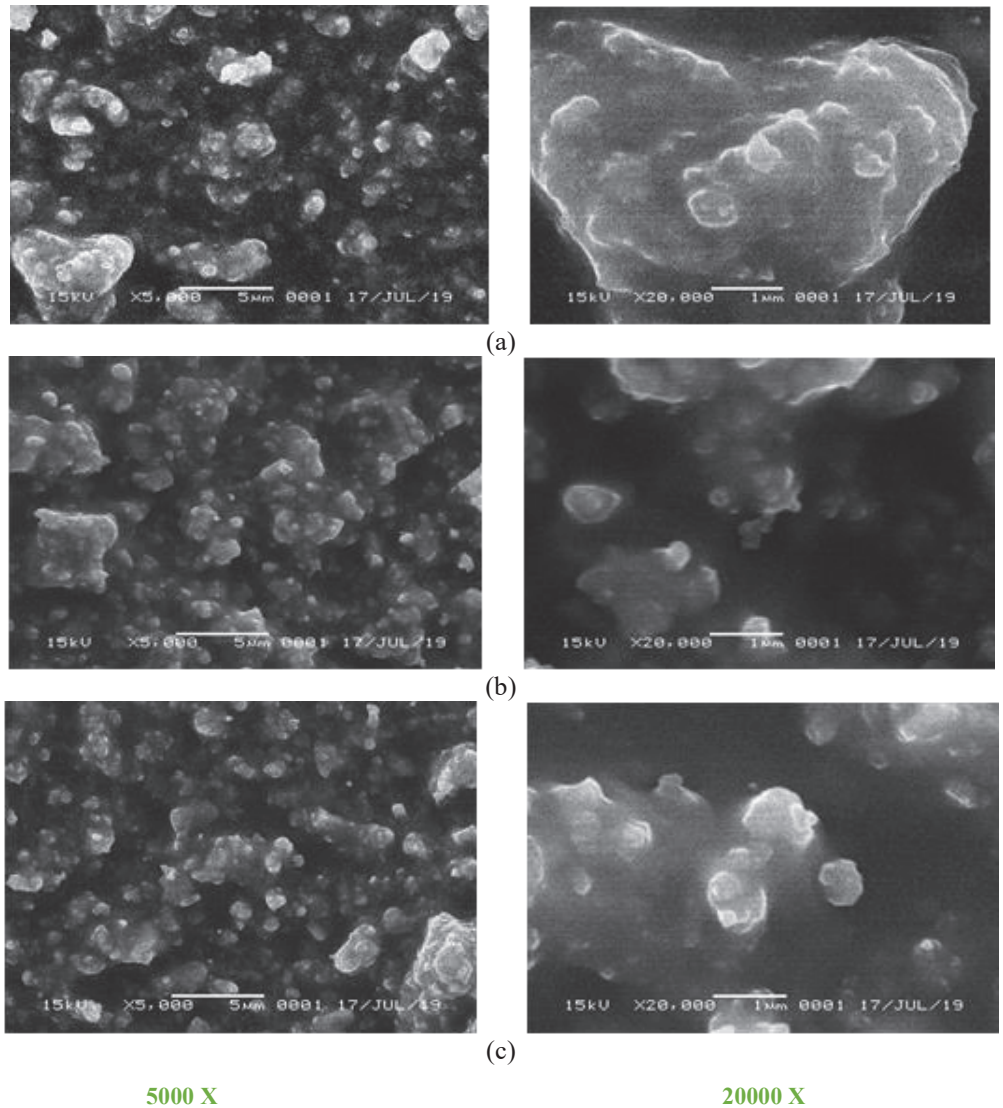

FIGURE 3. Scanning electron microscopic observation of all milled samples. (a) HM, (b) HC, and (c) HA

CONCLUSIONS

Carbonate apatite was successfully obtained from the mixture of HA powder from Center for Ceramic based on Indonesian limestone and carbonate source from $MgCO_3$ using dry mechanosynthesis. The mixture of materials was milling in a porcelain pot mill by the rotation speed of 80 rpm and interval 48 h. The results were charactered by XRD, FTIR, and SEM. The pattern peaks of XRD shows the apatite phase with sharp peaks around 31.6-33°. The grinding process and addition of carbonate ion cause decreasing in crystallinity. FTIR spectra indicate carbonate apatite type B is predominant, while type A was also detected in the weak peak. The morphology of samples was shown by SEM pictures and resulted in irregular shapes of particles consisting of finer agglomerates that interconnected into larger and different structures.

ACKNOWLEDGEMENT

This research was funded by the Center of Ceramic, Ministry of Industry, Republic of Indonesia.

REFERENCES

1. L.L.H. and S. Best, in *Biomater. Sci. An Introd. to Mater. Med.* (Academic Press, California, 1996).
2. P.W. Brown and B. Constantz, *Hydroxyapatite and Related Materials* (1994).
3. E. Landi, A. Tampieri, G. Celotti, L. Vichi, and M. Sandri, Biomaterials (2004).
4. J. Barralet, S. Best, and W. Bonfield, J. Biomed. Mater. Res. **41**, 79 (1998).
5. J. Barralet, M. Akao, and H. Aoki, J. Biomed. Mater. Res. **49**, 176 (2000).
6. A.A. Baig, J.L. Fox, J. Hsu, Z. Wang, M. Otsuka, W.I. Higuchi, and R.Z. LeGeros, J. Colloid Interface Sci. **179**, 608 (1996).
7. W.L. Suchanek, P. Shuk, K. Byrappa, R.E. Riman, K.S. TenHuisen, and V.F. Janas, Biomaterials **23**, 699 (2002).
8. S.A. Redey, M. Nardin, D. Bernache-Assolant, C. Rey, P. Delannoy, L. Sedel, and P.J. Marie, J. Biomed. Mater. Res. **50**, 353 (2000).
9. R. Tang, Z.J. Henneman, and G.H. Nancollas, J. Cryst. Growth **249**, 614 (2003).
10. K. Sawada, Pure Appl. Chem. **69**, 921 (1997).
11. T. Kato, Adv. Mater. (2000).
12. L. Qiao, Q.L. Feng, and Z. Li, Cryst. Growth Des. **7**, 275 (2007).
13. R.M.H. Verbeeck, E.A.P. De Maeyer, and F.C.M. Driessens, Inorg. Chem. **34**, 2084 (1995).
14. Y. Suetsugu and J. Tanaka, J. Mater. Sci. Mater. Med. **10**, 561 (1999).
15. Y. Suetsugu, Y. Takahashi, F.P. Okamura, and J. Tanaka, J. Solid State Chem. **155**, 292 (2000).
16. J. Coreño A., O. Coreño A., J.J. Cruz R., and C. Rodríguez C., Opt. Mater. (Amst). **27**, 1281 (2005).
17. R. Othman, N. Xuan, T. Tram, A. Fauzi, and M. Noor, **2**, 18 (2013).
18. D. Pham Minh, N.D. Tran, A. Nzihou, and P. Sharrock, Mater. Res. Bull. **51**, 236 (2014).
19. S. Kim and C.B. Park, Biomaterials **31**, 6628 (2010).
20. A. Bigi, E. Foresti, R. Gregorini, A. Ripamonti, N. Roveri, and J.S. Shah, Calcif. Tissue Int. **50**, 439 (1992).
21. A. Bigi, G. Falini, E. Foresti, A. Ripamonti, M. Gazzano, and N. Roveri, J. Inorg. Biochem. **49**, 69 (1993).
22. K.S. TenHuisen and P.W. Brown, J. Biomed. Mater. Res. **36**, 306 (1997).
23. R.Z. LeGeros, Monogr. Oral Sci. (1991).
24. Y. Yamasaki, Y. Yoshida, M. Okazaki, A. Shimazu, T. Uchida, T. Kubo, Y. Akagawa, Y. Hamada, J. Takahashi, and N. Matsuura, J. Biomed. Mater. Res. **62**, 99 (2002).
25. E. Landi, A. Tampieri, M. Mattioli-Belmonte, G. Celotti, M. Sandri, A. Gigante, P. Fava, and G. Biagini, J. Eur. Ceram. Soc. (2006).
26. M. Iafisco, A. Ruffini, A. Adamiano, S. Sprio, and A. Tampieri, Mater. Sci. Eng. C **35**, 212 (2014).
27. J. Sadło, L. Pajchel, J. Michalik, and W. Kolodziejski, J. Mol. Struct. **1022**, 61 (2012).
28. C. Suryanarayana, Prog. Mater. Sci. **46**, 1 (2001).
29. N.K. E. Avvakumov, M. Senna, *Soft Mechanochemical Synthesis: A Basis for New Chemical Technologies* (MA: Kluwer Academic Publishers, Boston, 2001).
30. H. El Briak-BenAbdeslam, M.P. Ginebra, M. Vert, and P. Boudeville, Acta Biomater. **4**, 378 (2008).
31. N.S. Kristanto Wahyudi, Frank Edwin, J. Keramik Dan Gelas Indones. **25**, 46 (2016).

32. F. Daitou, M. Maruta, G. Kawachi, K. Tsuru, S. Matsuya, Y. Terada, and K. Ishikawa, Dent. Mater. J. **29**, 303 (2010).
33. G.S. Kumar, E.K. Girija, A. Thamizhavel, Y. Yokogawa, and S.N. Kalkura, J. Colloid Interface Sci. **349**, 56 (2010).
34. S. Lala, M. Ghosh, P.K. Das, D. Das, T. Kar, and S.K. Pradhan, Mater. Chem. Phys. **170**, 319 (2016).
35. A. Zhu, Y. Lu, Y. Si, and S. Dai, Appl. Surf. Sci. **257**, 3174 (2011).
36. R.Z. LeGeros, O.R. Trautz, E. Klein, and J.P. LeGeros, Experientia (1969).
37. Q. He, Z. Huang, Y. Liu, W. Chen, and T. Xu, Mater. Lett. **61**, 141 (2007).
38. I. Rehman and W. Bonfield, J. Mater. Sci. Mater. Med. **8**, 1 (1997).